

# The fine structure of the Pleiades luminosity function and pre-main sequence evolution

A.N. Belikov<sup>1</sup>, S. Hirte<sup>2</sup>, H. Meusinger<sup>3</sup>, A.E. Piskunov<sup>1</sup>, and E. Schilbach<sup>2</sup>

<sup>1</sup> Institute of Astronomy of the Russian Acad. Sci., 48 Pyatnitskaya St., Moscow 109017, Russia  
(abelikov@inasan.rssi.ru; piskunov@inasan.rssi.ru)

<sup>2</sup> Astrophysikalisches Institut Potsdam, An der Sternwarte 16, D-14482 Potsdam, Germany (shirte@aip.de; eschilbach@aip.de)

<sup>3</sup> Thüringer Landessternwarte Tautenburg, Sternwarte 5, D-07778 Tautenburg, Germany (meus@tls-tautenburg.de)

Received 22 September 1997 / Accepted 27 November 1997

**Abstract.** The luminosity function (LF) of the Pleiades cluster stars was constructed for the study of the LF fine structure related to pre-MS stellar evolution. Theoretical luminosity functions based on present-day pre-MS and MS stellar models were constructed and compared with observations. We tested both power- and log-normal laws describing the cluster star IMF. Both single star formation burst- and age spread-models were examined. The agreement between the observed Pleiades CMD with the new HIPPARCOS distance and the theoretical ZAMS for a normal metallicity is excellent when the model positions in the HRD are corrected to the helium abundance  $Y=0.34$ . The corresponding age of the cluster is  $\log t = 7.95$ . Three features (dips) were found in the observed cluster LF in a magnitude range  $M_V = 5^m - 12^m$ . Two of them (at  $M_V = 7.5^m$  and  $9.5^m$ ) are assumed to be field LF features: Wielen and Kroupa dips. Theoretical models fail to reproduce them. We attributed the third (brightest) detail (the dip at  $M_V = 5.5^m$ ) to the pre-MS evolution of Pleiades stars. The observed Pleiades LF corresponds in its brighter part to the standard Population I IMF. The log-normal IMF fits the observations much better than a simple power-law IMF. The brightest LF feature could be reproduced in the theoretical LF if a substantial age spread of order of several tens of Myrs is supposed to exist among the Pleiades stars.

**Key words:** open clusters and associations: individual: Pleiades – stars: luminosity function, mass function – stars: pre-main sequence

---

## 1. Introduction

The nearby Pleiades open cluster has been a subject of numerous investigations over the decades. Its importance relies upon the cluster proximity and relative youth which make it a very

*Send offprint requests to:* E. Schilbach

valuable target of stellar evolution and star formation studies. Due to the small distance, deep observations provide a reliable kinematic membership determination down to faint magnitudes which is needed for the construction of luminosity and mass functions badly known at  $M_V \geq 5^m$  for the majority of other clusters.

The Pleiades became especially important for the pre-Main Sequence (pre-MS) evolution studies as their fainter stars were found still undergoing the gravitational contraction to the Zero-Age Main Sequence (ZAMS) (see e.g. Stauffer 1984). As Piskunov and Belikov (1996) did show, the presence of pre-MS stars in a cluster affects the cluster star luminosity function (LF), producing an additional detail in the LF. This LF feature depends on age, and according to Belikov and Piskunov (1997a), the Pleiades cluster occurs just at the edge of the age interval where this feature is still existent. Thus, it is worth to investigate the Pleiades where an accurate and complete LF is expected down to faint magnitudes from the point of whether this feature is seen in the cluster LF, and what could be learned about the cluster initial mass function (IMF) and the star formation rate (SFR) from the study of the Pleiades stars LF.

In the previous paper (Meusinger et al. 1996) the reliable LF of the Pleiades stars was constructed on the basis of a proper motion survey in the cluster central area, and converted to the mass function. It was found that the Pleiades stars mass spectrum has a turnover at about  $1m_\odot$ . In contrast, the present paper is concentrated on the study of the fine structure of the LF of Pleiades cluster stars related to the pre-MS stellar evolution. The theoretical LFs based both on post-MS and pre-MS present-day stellar models were constructed and compared with observations.

In Sect. 2 we describe input data we used: observations, their reduction, cluster membership, evolutionary tracks and scales of effective temperatures and bolometric corrections implemented. An analysis of the resulting Pleiades color-magnitude diagram and the observed LF is given in Sect. 3. We construct theoretical LFs and compare them with the observations in Sect. 4. The

main results are given in Sect. 5 and, finally, in Sect. 6 we draw conclusions.

## 2. Input data

### 2.1. Observations and data

An essential part of the observations for the proper motion survey was obtained with the Tautenburg Schmidt telescope (134/203/401) between 1961 and 1992. Eleven partly overlapping plate pairs with epoch differences from 23 to 30 years cover a total region of about 17 square degrees centered near Alcyone. Additionally, three second epoch Tautenburg plates were also included in the programme. In contrast to our previous proper motion determination based on these data (Meusinger et al. 1996), we added further 14 Astrographic Catalogue plates (Paris and Oxford zones) with observational epochs from 1891 to 1909.

The photometric survey is based on Tautenburg plates and plates taken with the Schmidt telescope (90/152/316) of the Observatoire de la Côte d’Azur (OCA). The observations, plate measurements and data reduction for the determination of the photographic B, V and R magnitudes as well as the discussion of the survey completeness are given in Meusinger et al. (1996).

### 2.2. Reductions

A central field of the proper motion survey of about 5.5 square degrees is overlapped by all 25 Tautenburg plates whereas field edges of 2 square degrees in total are covered only by one plate pair. The proper motions were determined for stars which were detected at least on one first and one second epoch Tautenburg plate. Additionally, there are at least two AC observations for stars brighter than  $14^m$ .

To derive proper motions of the measured stars, we used the block-adjustment of overlapping plates by Eichhorn (1960). In this method the plate constants as well as the star constants – positions and proper motions – are regarded as unknowns in one least squares solution. In contrast to the usual plate-to-plate reduction, this approach allows to derive proper motions in a common reference system. With the AC measurements in the solution, the proper motion accuracy of stars brighter than  $V = 14^m$  could be increased simply by a longer time base. On the other hand, as the AC stars are distributed over the whole field of the survey, a better accuracy of bright stars improves the proper motion system and, consequently, the systematic accuracy of proper motions of faint stars becomes also better. Because of the very large system of equations (about 1 000 000 equations for 200 000 unknowns), an iterative solution was used where plate constants and star constants are determined alternatively.

The PPM was chosen as a reference catalogue. Altogether 269 PPM-stars were used to derive first estimates of the plate constants. On each Tautenburg plate we had 104 to 129 PPM-stars and on an AC-plate between 12 and 87 PPM-stars depending on the percentage of overlap with Tautenburg plates. Therefore, we used a second order polynomial for the Tauten-

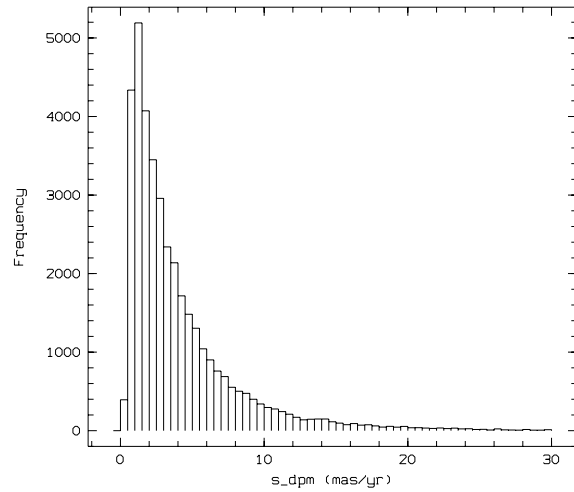


**Fig. 1.** Histogram of the proper motion errors in declination (similar for right ascension).

burg and a first order polynomial for the AC-plates. With these plate constants, positions and proper motions were determined.

After the first iteration systematic errors in the proper motions were found. They are caused by the random errors of the catalogue. Therefore, a new catalogue was constructed containing all stars with accurate positions and proper motions smaller than 25 mas/yr and the reduction was newly started. For the new computations only the positions of the new catalogue were used assuming that all proper motions are zero. Now sixth order polynomials were applied for Tautenburg and first order polynomials for AC-plates. After 20 iterations the solution became stable and did no more show the systematic effects (Röser et al. 1995).

The proper motion survey includes about 40 000 stars. Fig. 1 shows the histogram of proper motion errors in declination as an example of the final accuracy of the solution.

### 2.3. Pleiades membership

In order to obtain the final member list, both kinematic and photometric selection procedures were applied to the data. These procedures considered loci of stars in the proper motion vector point diagram (VPD) and in the color-magnitude diagram (CMD). The selection was carried out in several steps.

Whereas the bulk of field stars in the VPD are concentrated towards the point  $\mu_\alpha = 0$  mas/yr,  $\mu_\delta = 0$  mas/yr, the Pleiades show a clear concentration toward the center of their distribution at  $\mu_\alpha = 16$  mas/yr,  $\mu_\delta = -42$  mas/yr. At the first step, we considered all stars around this point inside a circle with a radius of 25 mas/yr as preliminary cluster candidates. Due to significantly higher proper motion errors of stars with  $V \geq 18$ , the selection radius for faintest members in our sample was increased to 27.5 mas/yr. This preliminary proper motion selection yielded 1585 candidates including 234 stars with only V and R magnitude measurements. The most of the stars from the latter group belong to the faintest objects ( $V > 17$ ) in the survey

which were not detected on B plates limited at  $B = 18 - 19$  mag. For each candidate, the proper motion membership probability  $p_{pm}$  was computed in accordance with the method described in Meusinger et al. (1996) using information on proper motion error distribution over magnitude and location of objects in the VPD.

As the second step, the following procedure was used for the photometric selection of the Pleiades members. The Pleiades candidates with the highest proper motion membership probabilities ( $p_{pm} > 60\%$ ) and with available photoelectric photometry were used to construct their  $V, (B - V)$  diagram. The diagram shows a clear cluster MS with a sharply defined blue edge. This “blue envelope” was quantified as a representative of the cluster ZAMS. Photometric membership probabilities  $p_{ph}$  were derived from the location of the preliminary candidates relative to the cluster MS taking into account the photometric accuracy of the data.

All Pleiades candidate stars having  $B - V$  colors (1346 stars) were passed through the “photometric” filter. For the cluster candidates, the color deviation out of the blue envelope was computed. The stars to the right of the envelope were considered as the photometric cluster candidates with the highest photometric probability. All stars which deviate blue-ward out of the envelope further than  $3\sigma_{B-V}$  were classified as field stars (i.e. zero photometric probabilities).

The final selection was carried out in the third step by the combining of the photometric and proper motion probabilities. We rejected from the cluster candidate list those stars which got one of the probabilities equal to zero. The stars with  $p_{pm} < 1.5\%$  and  $p_{ph} < 1.5\%$  (i.e. deviations larger than  $2.5\sigma$ ) were excluded from the sample, too. Generally, the astrometric and photometric criteria showed a good coincidence. For a few critical cases, an additional analysis was necessary considering also individual proper motion and color errors. This step yielded 629 Pleiades candidates.

Since 239 faint candidate stars have no  $B - V$  colors, the previous considerations could not be applied. We used the following procedure for these stars. The  $V, V - R$  diagram was constructed for definite Pleiades members selected at the previous step, which have both  $B - V$  and  $V - R$  colors. The positions of 239 faint member candidates were compared with definite member positions in the  $V, V - R$  diagram. The similar procedures as described in two previous steps were applied. As a result, 108 additional cluster candidates were selected.<sup>1</sup>

For 43 bright well established Pleiades members no reliable data could be obtained from Schmidt plate measurements. These stars were added to the sample with data taken from the literature. The sample defined by the photometric and proper motion constraints includes 780 Pleiades members in total.

<sup>1</sup> The complete data on 737 cluster candidates with positions, proper motions, photographic magnitudes, membership probabilities, and cross-identifications are available at cdsarc.u-strasbg.fr (CDS) via anonymous ftp. They are also stored in the Base des Amas (BDA).

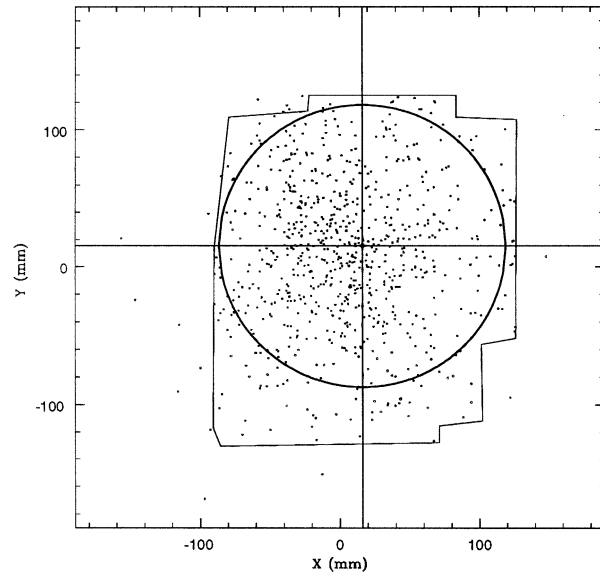


**Fig. 2.** Distribution of 780 Pleiades members in x,y-plane. The broken line indicates the area covered by the proper motion survey limits. The cross of lines corresponds to the cluster center ( $\alpha_c, \delta_c$ )<sub>J2000.0</sub> = ( $3^h 47^m 53^s, 24^\circ 15.6'$ ) derived by star counts. The circle is the edge of the area where the final list of Pleiades members was selected from. Scale is  $65.25''/mm$ .

#### 2.4. Final sample

The proper-motion survey covers a quite irregularly shaped area (Fig. 2). This may lead to selection effects, e.g. due to the well-known fact of mass segregation. In order to avoid a possible bias, we have selected Pleiades members only which fall inside the maximum circle around the cluster center (see Fig. 2). The cluster center was determined from star counts at ( $\alpha_c, \delta_c$ )<sub>J2000.0</sub> = ( $3^h 47^m 53^s, 24^\circ 15.6'$ ). The radius of the circle is 111.68 arcmin. Altogether, there are 647 cluster members within this circle. We use this sample throughout the paper.

#### 2.5. Adopted parameters

The distance modulus  $V_0 - M_V = 5.33^m$  as derived by HIPPARCOS parallax observations (Mermilliod et al. 1997) was applied with the color excess  $E(B - V) = 0.06^m$ , which is close to  $E(B - V) = 0.053^m$  from Crawford and Perry (1976) and to the standard value of  $0.04^m$  (Meusinger et al. 1996).

#### 2.6. Evolutionary tracks

In order to construct theoretical isochrones and LFs which include both post-MS and pre-MS stages for ages typical to that of the Pleiades (about 100 Myrs), we combined Population I pre-MS evolutionary tracks of D’Antona and Mazzitelli (1994) and Maeder group post-MS calculations (Schaller et al. 1992). We selected the MLT convection and Alexander opacities subset of D’Antona and Mazzitelli tracks which is in the best agreement with observations of M-dwarf binaries (Malkov et al. 1997).

Both systems were properly tuned to provide continuous transition from pre- to post-MS ages at the same mass as well as smooth and uniform mass-luminosity and mass-radius relations along the ZAMS.

To conform the new Pleiades color - absolute magnitude diagram (i.e. the new trigonometric parallax distance modulus, derived by HIPPARCOS) with the theoretical ZAMS for normal metallicity ( $Z=0.02$ ), the helium abundance which fits the cluster ZAMS best ( $Y=0.34$ ) was derived. The model positions in the theoretical HRD were corrected for the difference between the original model helium content and the “best” Pleiades  $Y$ -value of 0.34 according to

$$\begin{aligned}\Delta \log L &= -7.8 \Delta \log(1.997 - \frac{5}{4}Y), \\ \Delta \log T_{eff} &= -2.2 \Delta \log(1.997 - \frac{5}{4}Y)\end{aligned}$$

valid for pp-cycle and  $Z = 0.02$  (see Sears and Brownlee 1965). It should be stressed that there is no direct observational evidence supporting such a high helium abundance of Pleiades stars. But in absence of a general idea how to remove a discrepancy of order of  $0.5^m$  between the Pleiades and Presepe group clusters main sequences (see Mermilliod et al. 1997), we used helium abundance as a free parameter to provide the fine adjustment of the observed and theoretical CMDs. We can state that with the corrections applied the agreement between the theoretical and the observed CMD became even better, than it was with older distance and normal helium abundance.

The isochrones were interpolated from the track system according to the technique described by Belikov and Piskunov (1997b).

### 2.7. Scales

In order to convert theoretical coordinates of the Hertzsprung-Russell diagram,  $\log T_{eff}$ ,  $\log L/L_{\odot}$ , to the observed ones,  $(B - V)_0$ ,  $M_V$ , we used bolometric corrections and  $(B - V) - \log T_{eff}$  relations from Schmidt-Kaler tables (1982) for the luminosity classes I, III and V.

### 3. Analysis of observational data

The color-magnitude diagram of the sample is shown in Fig. 3. Due to high quality photometric data, the Pleiades main sequence is clearly outlined. The lower envelope at  $M_V$  from  $1^m$  to  $6^m$  evidently coincides with the ZAMS. At brighter magnitudes up to the MS turn-off point at  $M_V = -3^m$  stars are already evolving off the ZAMS. Stars fainter than  $M_V = 6^m$  are lifted above the ZAMS and follow rather pre-MS isochrones, than the ZAMS. As isochrones show, the turn-on point is located within the  $M_V$  interval from  $5^m$  to  $7^m$ . The upper MS envelope also being clearly defined by accurate data presumably indicates the equal mass unresolved binaries sequence. Lower quality photographic data show a definite scattering around the ZAMS, which could be attributed to higher photometric errors of photographic magnitudes. The scattering increases toward faintest magnitudes and reaches the maximum value at  $M_V$  from  $10^m$  to

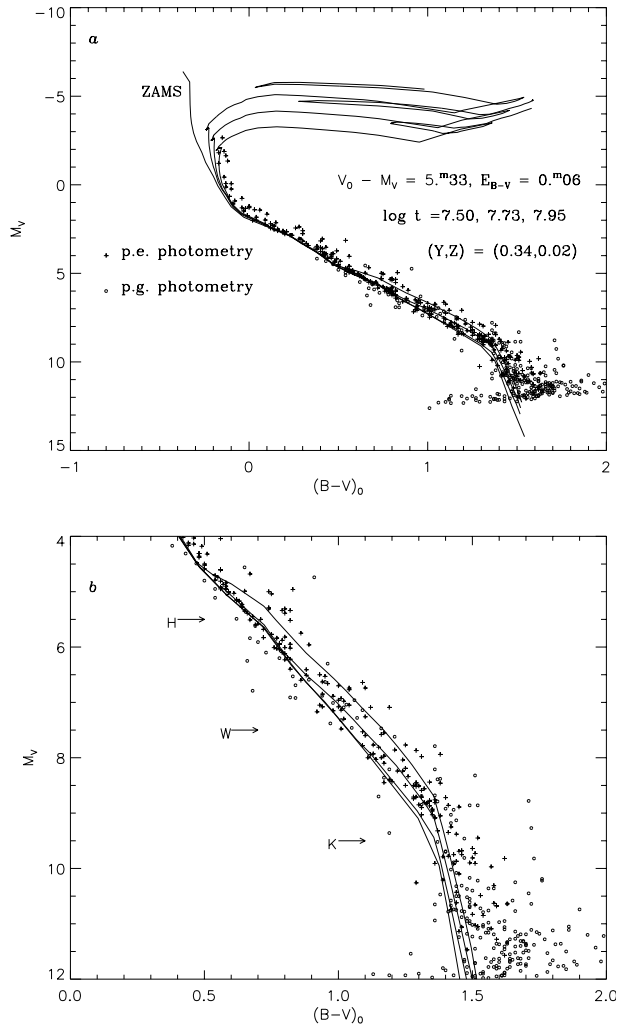


**Fig. 3a and b.** Color - magnitude diagram of the Pleiades sample. Panel **a**: all stars, panel **b**: Pre-MS portion. Plus signs indicate the members with the high quality photometry, open circles are those with photographic magnitudes. The line denoted as “ZAMS” is the used theoretical ZAMS. The isochrones of  $\log t = 7.50, 7.73, 7.95$  for both post-MS, and pre-MS stages are also shown.

$12^m$ . For the adopted distance modulus and color excess, theoretical data are in good agreement with observed points for both upper and lower MS.

In order to reveal details of the Pleiades LF, we have to use a technique more sophisticated than a histogram construction. We used the kernel estimation method with the simplest “naive” (rectangular) kernel (see Silverman (1986) for more details of the method)

$$\phi(M_V) = \sum_i K\left(\frac{M_V - M_{Vi}}{h}\right)$$

where

$$K(x) = \begin{cases} 1, & |x| < 1.0 \\ 0, & |x| \geq 1.0 \end{cases}$$

and  $i$  goes through the data sample.

The smoothing procedure was applied to the theoretical LF with the same “naive” kernel as for the observed LF. The smoothing parameter  $h = 1.0^m$  and step  $\Delta M_V = 0.05^m$  were used in calculations. From numerical tests with our data sample we found that a larger smoothing parameter ( $h = 2.0^m$ , for instance) oversmooths the resulting LF while  $h < 1.0^m$  under-smooths.

The empirical LFs in  $M_V$  for defined Pleiades members and non members in our preliminary sample of 1585 cluster candidates are shown in Fig. 4. The clear difference between the distributions confirms the correctness of the selection procedure. As the proper motion survey is complete down to  $V = 17^m$  (Meusinger et al. 1996), we considered the LF as reliable in the absolute magnitude  $M_V$  range from  $-3^m$  to  $11^m$  and concluded that all structural details within this interval reflect the real behaviour of the LF. We considered the LF drop at  $M_V \geq 11^m$  as a possible incompleteness at fainter magnitudes.

The Pleiades LF obviously consists of several sections. The first one ( $M_V < 5^m$ ) is, in fact, the MS LF portion and reveals the behaviour typical for young open cluster LFs. The second portion ( $5^m < M_V < 10^m$ ) represents a plateau with three dips at  $M_V = 5.5^m$ ,  $7.5^m$ , and  $9.5^m$ . The first dip together with the adjacent maximum has a pre-MS nature and is discussed in Sect. 4. The fainter dips could be identified with the features known from the field star LF: the well established Wielen dip ( $M_V = 7.5^m$ ) and a dip which was discussed first by Kroupa et al. (1990). To our knowledge, this is the first time when both of these field star LF features were discovered in a star cluster LF also. All these dips could be also seen in the Pleiades CMD (see Fig. 3b). The last LF section ( $M_V > 10^m$ ) is a domain of further increase of the LF. Unfortunately, due to the survey limit we could not safely realize how steep the slope of the faint LF is and where the LF turnover point will be reached.

In order to evaluate independently the statistical significance of the proposed dips in the LF, we performed a series of Monte Carlo experiments with a probability distribution function equal to a raw luminosity function shown in Fig. 4a and with a suitable photometric error distribution with stellar magnitude. We removed consequently from the LF the proposed dips to prove whether they could appear as a result of small number statistics. As the simulations showed, the existence of the gaps could not be rejected at 87% confidence level for the first feature, 94% level for Wielen dip, and 98% level for Kroupa et al. dip. Furthermore, we applied Monte Carlo simulations as described by Meusinger et al. (1996) to study the effect of a correction for unresolved binaries. In general, such a correction will slightly smooth out the observed LF fine structure. However, the resulting LFs showed clearly the three dips in 95 out of 100 simulation runs.

#### 4. Theoretical LFs: construction and comparison with observations

As it is well known, the LF depends on both the initial mass function and the mass-luminosity relation (MLR) derivative (i.e.

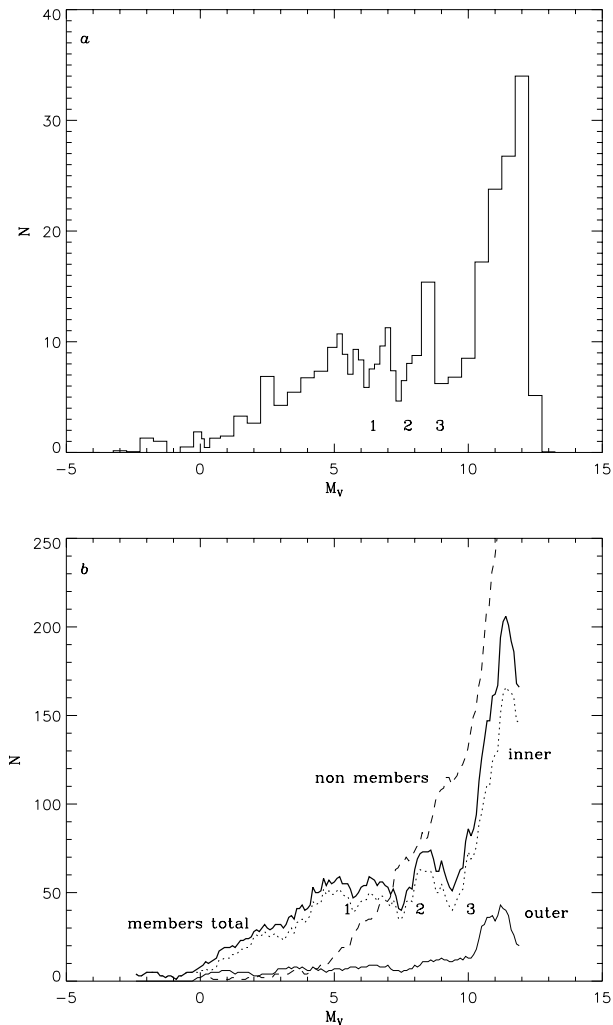


**Fig. 4a and b.** The observed Pleiades LFs. Panel **a**: raw LF, binned in 0.2 mag. boxes, panel **b**: smoothed LFs. Thick continuous line for all members, dotted curve - “inner” members (i.e. located inside the circle in Fig. 2), thin continuous line - “outer” members (i.e. located outside the circle in Fig. 2), dashed line - non member stars assuming the same distance as for the Pleiades. 1 - MS/pre-MS transition dip, 2 - Wielen dip, 3 - Kroupa et al. (1990) dip.

the slope of the mass-luminosity relation). Therefore, since the MLR of pre-MS stars differs from that of MS stars, the pre-MS branch (in clusters where it is present) should affect the LF. Especially, a sharp contrast is expected at (or just below) the turn-on point at the transition between MS and pre-MS branches. According to Piskunov and Belikov (1996), this transition produces a local “bump” in the LF followed by a dip (herein we call this “bump” as “H-peak” and the effect of peak and dip existence as “H-feature”. We choose this abbreviation to stress that the feature is related to the beginning of hydrogen burning as a star approaches the ZAMS).

Since the turn-on point luminosity depends on age, the position of the H-feature in the LF also evolves with time to lower luminosities. The amplitude of the “bump” does not change sig-

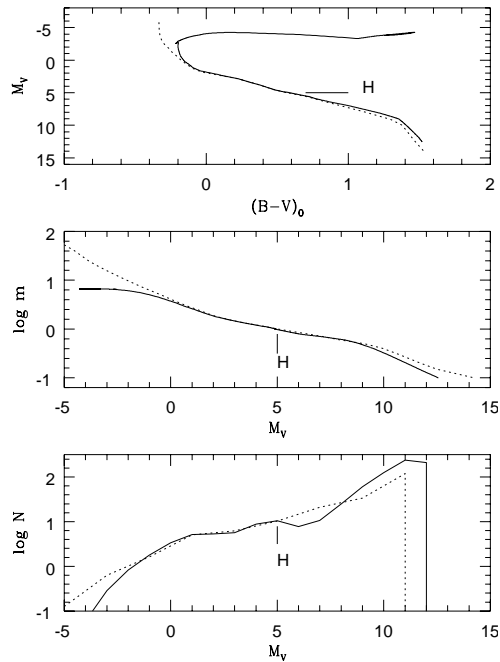


**Fig. 5.** An illustration of the origin of the H-feature in the LF of the coeval cluster of age  $\log t = 7.7$ . H marks the position of turn-on point and the related details, continuous lines correspond to the isochrone, dotted lines to the ZAMS. Panels: at the top are theoretical color - magnitude diagrams, in the middle are mass - luminosity relations and at the bottom are LFs.

nificantly, while the dip gradually narrows. By an age of 100 - 120 Myrs the feature disappears due to the fact that the turn-on point enters the region of stars with  $m < 0.6m_{\odot}$  whose luminosities decrease monotonically as they approach the ZAMS.

In Fig. 5 we show the theoretical CMD, the corresponding  $M_V - \log m$  relations and the LFs (a) for a coeval artificial star cluster of age  $\log t = 7.7$  and for (b) a hypothetical cluster where all stars are on the ZAMS. There is no fine structure in the ZAMS-LF but there is a strong bump-dip feature in the LF for  $\log t = 7.7$ . This structure is attributed to the pre-MS evolution and, therefore, can be identified with the H-feature. Note also that the used stellar model data do not reproduce the Wielen-dip and the Kroupa-dip in the ZAMS-LF.

There are several evidences coming from the Pleiades CMD analysis (e.g. Meynet et al. 1993; present study) as well as from the independent analysis of Li contents in Pleiades faintest stars (Basri et al. 1996) that the cluster age is about 100 Myrs. For this age we can expect the transition between MS and pre-MS stars at  $M_V \approx 5^m$ . This is confirmed by the cluster CMD for accurate photometric data (see Fig. 3). This fact allows us to attribute the first of the dips in the empirical LF discussed in Sect. 3 to the H-feature. The position of the H-peak in magnitude scale is in a reasonable agreement with its predicted position from the theoretical age-H calibration (Belikov and Piskunov 1997a) for the Pleiades age. The H-maximum is quite small and the dip is narrow but clearly visible.

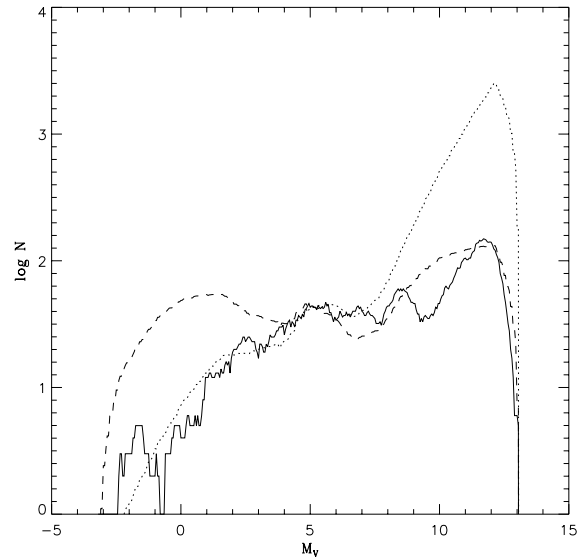


**Fig. 6.** Illustration of the “fitting range” effect. Continuous line - observed LF. Theoretical luminosity functions for  $\log t = 7.72$  and power-law IMF: dotted line - fitting over  $-3^m \leq M_V \leq 7^m$  with the resulting  $x = 1.55$ ; dashed line - fitting over  $-3^m \leq M_V \leq 12^m$  with the resulting  $x = 0.20$ .

As we mentioned above, the present-day pre-MS models forecast that the H-feature should disappear or be considerably diminished at the age of the Pleiades. Therefore, assuming that the models by D’Antona and Mazzitelli (1994) are correct, we should not observe a prominent H-feature in the Pleiades LF. Then, the only possibility to keep the H-feature in the theoretical LF at the Pleiades age with the used pre-MS models is to suppose that a substantial amount of the Pleiades stars is younger than the 100 Myrs, i.e. there is an age spread in the cluster. Generally, an age spread among the stars of a younger cluster does not influence the H-feature significantly, smoothing it a little. In contrast, at ages, comparable with that of the Pleiades, the age spread reduces the mean age of the cluster stars to a value where the H-feature is detectable (see Fig. 7). Therefore, the existence of an H-feature in the Pleiades LF can be regarded as an evidence for the hypothesis of age spread among the cluster stars, provided that the used theoretical isochrones are correct.

This enables us to construct the Pleiades theoretical LF reproducing the detected feature and to draw conclusions on the cluster IMF, and, possibly, on the star formation history in the cluster. The theoretical LF  $\phi(M_V)$  was calculated according to

$$\phi(M_V) = \int_{t_0}^{t_1} \phi_t(M_V) \lambda(t) dt$$

where  $t_0$  and  $t_1$  are minimum and maximum ages of the cluster stars,  $\phi_t(M_V)$  is the LF of stars with age  $t$  ( $t_0 \leq t \leq t_1$ ),  $\lambda(t)$  is the star formation rate at which stars with age  $t$  were formed. The time integration step was properly adjusted to avoid artificial non-monotonous features in  $\phi(M_V)$  and conforms the condition  $\delta \log t \leq 0.1$ .

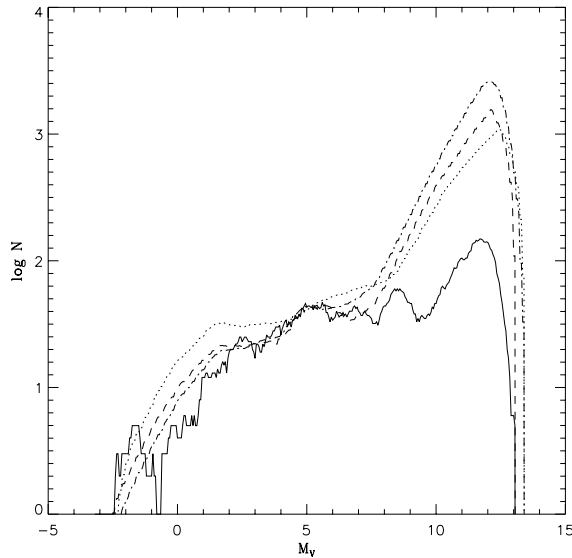


**Fig. 7.** Illustration of the age spread effect on the luminosity function for a power-law IMF. Continuous line - observed luminosity function. Dotted-dashed line - the theoretical LF of an artificial cluster with continuous SFR and maximum star age of  $\log t = 7.95$ . The SFR duration is 57 Myrs (the average age is  $\log t = 7.72$ ),  $\beta = 0.31$ , and the resulting  $x = 1.58$ . Theoretical luminosity functions of coeval cluster stars for  $\log t = 7.72$ ,  $x = 1.55$ , and  $\log t = 7.95$ ,  $x = 1.08$  are shown by dashed and dotted lines, respectively.

For  $\phi_t(M_V)$  we have:

$$\phi_t(M_V) = \left. \frac{dN}{dM_V} \right|_t = f(\log m[M_V, t]) \left. \frac{d \log m}{dM_V} \right|_t$$

where  $f(\log m) = dN/d \log m$  is the IMF. The mass- $M_V$  relation  $m(M_V, t)$  and its derivative were calculated along the isochrone of age  $t$  by use of cubic spline interpolation.

We considered two representations of the IMF:

- a power-law  $f(\log m) = km^{-x}$
- a log-normal law  $f(\log m) = e^{(c-a \log m - b \log^2 m)}$

where  $k$ ,  $x$ , and  $a$ ,  $b$ ,  $c$  are parameters.

For the SFR we assumed a power-law approximation in the form:

$$\lambda(t) = t^\beta$$

where  $\beta$  is a parameter.

As result, we obtained a set of parameters for the IMF ( $x$  for power-law or  $a$ ,  $b$  for log-normal) and SFR ( $\beta$ ), and minimum and maximum ages ( $t_0$ ,  $t_1$ ) for the cluster which could be computed by the minimization of the theoretical and observed LFs square deviations. Since we arbitrarily normalized the theoretical LF at  $M_V = 5^m$ , the IMF normalization parameters  $k$  and  $c$  were not determined. Before the fitting procedure was applied, both theoretical and observed LFs were passed through the “naive” filter.

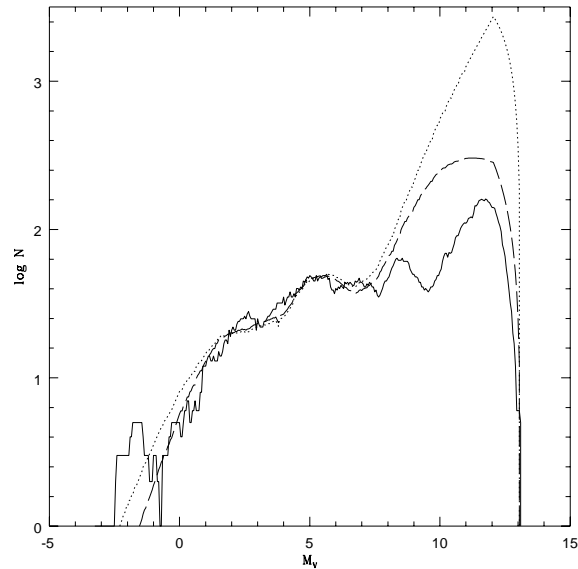


**Fig. 8.** Illustration of the IMF shape effect on the luminosity function. Continuous line - observed LF. Theoretical LFs for coeval clusters of an age of  $\log t = 7.72$ : dotted line - power-law IMF with resulting  $x = 1.55$ ; dashed line - log-normal IMF with the resulting  $a = 3.25$ ,  $b = 2.20$ .

We used the simplest least-squares minimization procedure to fit theoretical and observed LFs. Two parameters were derived as a measure of the fit quality:  $s$ , the sum of square deviations between the fitted LFs, and  $\Delta$ , the difference between H-maxima positions for theoretical and observed luminosity functions within the fit interval. The minimization of  $s$  and  $\Delta$  proceeded in several subsequent steps. First, the average age of the cluster was determined by fitting the positions of observed and theoretical H-peaks. The age spread for cluster stars was obtained in the next step. The IMF slope (or the IMF parameters in the case of log-normal mass function) was determined in the third step, and the SFR slope ( $\beta$ ) was computed at last. Initially, the full range of available absolute magnitudes ( $-3^m \leq M_V \leq 12^m$ ) was used for the LFs fitting. However, as we found, the theoretical tracks we used cannot reproduce the fainter features of the observed LF, i.e. Wielen and Kroupa et al. (WK for shortcut) dips. Therefore, we restricted our final computation to a narrower magnitudes interval ( $-3^m \leq M_V \leq 7^m$ ), which, for certain, contains the H-feature.

## 5. Results and discussion

In Figs. 6 to 8 the influence of the effects mentioned above on the LF is shown. Fig. 6 presents the fitting range effect for the power-law IMF and coeval SFR. Although the complete range fitting does correctly reproduce the LF behaviour at faintest magnitudes, it fails to reproduce the LF behaviour at brighter portion of the LF. Fig. 7 illustrates the effect of age spread on the H-feature for the case of a power-law IMF. The theoretical LFs were computed both for coeval and non-coeval stars. As we already mentioned, the age spread causes a smoothing of the H-feature. Finally, in Fig. 8

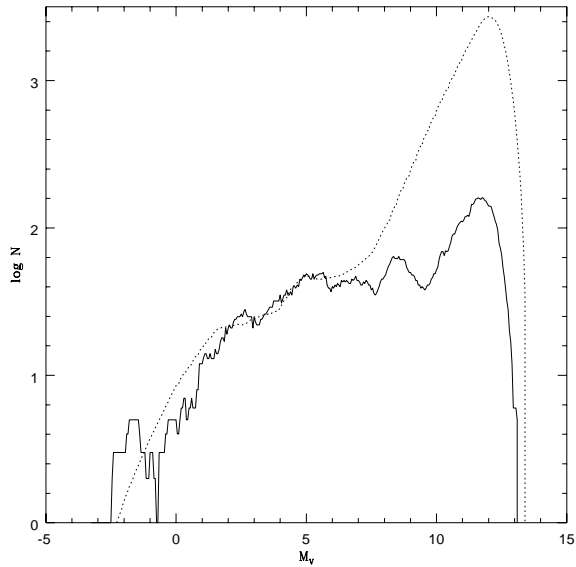


**Fig. 9.** “Single IMF” approximation for the power-law IMF (case P1 in Table 1). Continuous line - observed LF. Dotted line - theoretical LF (see Table 1 for the parameter values).

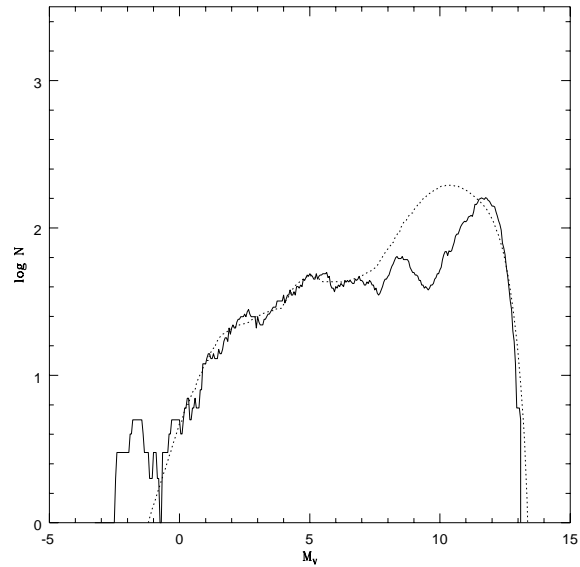


**Fig. 10.** “Single IMF” approximation for the log-normal IMF (case L1 in Table 1). Continuous line - observed LF. Dotted line - theoretical LF (see Table 1 for the parameter values).

the effect of the IMF shape on the LF is shown. The theoretical LFs were calculated for both the power-law and log-normal IMFs in coeval SFR approximation. According to Fig. 8, both IMFs are equal in description of the H-feature. The log-normal IMF produces a LF which is much closer to observations at faint magnitudes ( $M_V \geq 8^m$ ) but is under-abundant at brightest magnitudes ( $M_V < -1^m$ ).

The other important effect which may influence the LF comes from unresolved binaries (UBs). As noted already, the observed CM diagram is affected by binaries and the question arises, whether also the LF shape could be significantly influenced by the binaries. This problem was considered by Piskunov & Malkov (1991), and Meusinger et al. (1996). As these studies showed, the effect is relatively small in the absolute magnitude range considered in the present paper. Piskunov & Malkov (1991) compared the LFs of UBs and their components. They found that the effect of UBs depends on the binaries mass ratio distribution and reaches its maximum for a distribution which peaks at unity. Even in this case, the UBs do not much change the shape of the LF, but displace the whole LF by  $0.75^m$ . The other mass ratio distributions produce much smaller effects, although, the LF will become slightly smoothed after correction. It should be noted that the mass ratio distribution of field binaries in the solar neighbourhood does not show a maximum probability for equal mass binaries (Duquennoy & Mayor 1991). Meusinger et al. (1996) have used Monte Carlo simulations to investigate the effect of UBs on the Pleiades LF. They also did find that binaries have a minor effect on the shape of the Pleiades LF. This is the reason why the UBs have not been considered in more detail in the present paper. This conclusion could be changed if the mass ratio distribution or the fraction of UBs depend on the absolute magnitude, causing thus an effect depending on star

brightness and affecting to some degree the LF shape. However, we consider this situation to be highly improbable.

Monte Carlo simulations (cf. Sect. 3) have shown that the fine structure of the LF is affected by the correction for UBs: The significance of the H-feature is reduced when binarity is taken into account. However, the effect is only moderate and the H-feature was found to be still detectable in the overwhelming majority of the simulated LFs after binary correction. Nevertheless, we agree with the referee (J.R. Stauffer), that the correction for UBs has the tendency to reduce the need for a strong age spread. It would be important to have more data on binaries in the Pleiades and more realistic simulations to understand whether the H-feature may be significantly influenced by UBs.

Figs. 9 to 12 summarize the main results of this study. The non-coeval SFR is adopted in all the cases. The results of the fitting procedure are given in Table 1 together with the corresponding  $s$  parameters ( $\Delta = 0$  was achieved in all cases).

In Figs. 9 and 10 we show a “single” IMF approximation for the power-law (P1 in Table 1) and log-normal (L1) IMFs. We can conclude that the best fit is obtained with the log-normal IMF. Again, the “power-law” LF forecasts too much faint stars. Although the “log-normal” LF underestimates the brightest stars, in total, the agreement with observations within the fitting interval is much better than with the “power-law” LF. On the other hand, the WK-features are not seen in the theoretical LF, independent of which IMF was used. Therefore, we assume that these features are rather due to the mass- $M_V$  relation than to the IMF itself.

In the study of the low-luminosity stellar mass function Kroupa et al. (1990) discussed possible mechanisms causing the WK-dips. They proposed that both details of the LF are the result of the mass-luminosity relation fine structure generated

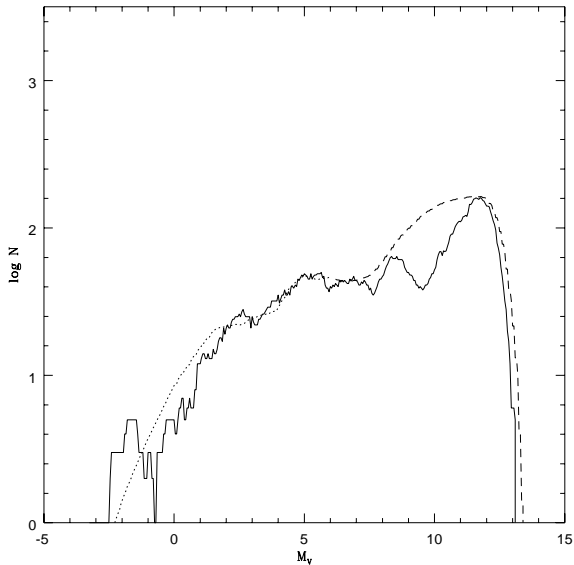


**Fig. 11.** “Two-section IMF” approximation for the power-law IMF (case P2 in Table 1). Continuous line - observed LF. Dotted line - Sect. 1, dashed line - Sect. 2 of the theoretical LF (see Table 1 for the parameter values).

by the equation of state and the opacity law. They proved this idea by computing low-mass ZAMS models and showed that the Kroupa et al. dip is caused by the influence of  $H_2$  molecules on the equation of state. They attributed the Wielen dip to the increasing importance of  $H^-$  ions as an opacity source. Unfortunately, the more sophisticated models of D’Antona and Mazzitelli (1994) used in the present study do not reproduce these details.

Since the “single” power-law IMF approximation fails to describe the behaviour of the observed LF at faintest magnitudes (for  $M_V$  from  $10^m$  to  $12^m$ ), we considered a “two-section” approximation for the power-law mass function. For comparison, the two-section approximation was applied to the log-normal IMF as well. The first section covers a magnitude range from  $-3^m$  to  $7^m$  for both power-law and log-normal IMFs. We did not fit the fainter magnitudes LFs precisely in the second section, rather we tried to reproduce the general increase of the observed LF between  $M_V = 7^m$  and  $12^m$  by an appropriate power law. As necessary estimates showed, the proper power index of this section is  $x = 0.10$ . In Fig. 11 we compare the “power-law + power-law” theoretical (P2 in Table 1) and observed LFs. In this case, the qualitative agreement with observations is improved. In Fig. 12 “log-normal + power law” (LP in Table 1) the theoretical LF is shown. This approximation does not differ significantly from L1 case (pure log-normal approximation).

From our results a continuous star formation taking a considerable fraction of the cluster history is required to reproduce the observed H-feature. We tested the SFR duration effect and found that at the given Pleiades age the H-feature is marginally visible at  $t_1 - t_0 \approx 18$  Myrs. When we tried to decrease the SFR duration we obtained unrealistic values for  $x$  (or  $a$ ,  $b$ ) and

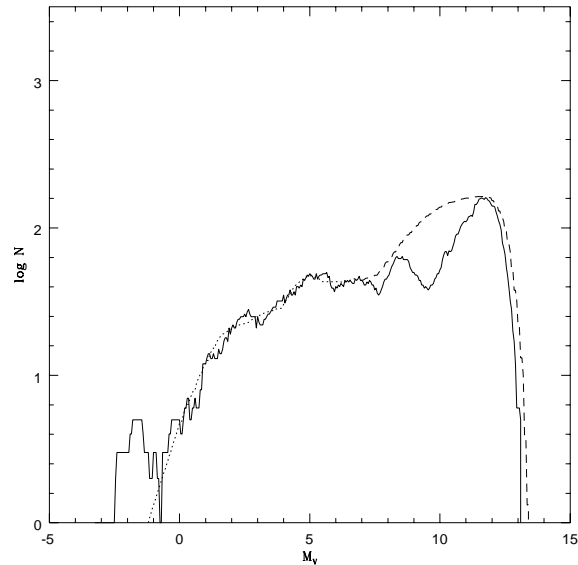


**Fig. 12.** “Two-section IMF” approximation for the log-normal IMF (case LP in Table 1). Continuous line - observed LF. Dotted line - Sect. 1, dashed line - Sect. 2 of the theoretical LF (see Table 1 for the parameter values).

**Table 1.** Results of the fitting procedure in a  $M_V$  magnitude range from  $-3^m$  to  $7^m$ .

case	$\log t_0$	$\log t_1$	$\beta$	a	b	x1	x2	s
P1	7.5	7.95	0.0	-	-	1.57	-	56.0
L1	7.5	7.95	0.15	3.15	3.30	-	-	36.2
P2	7.5	7.95	0.0	-	-	1.57	0.10	56.0
LP	7.5	7.95	0.15	3.15	3.30	-	0.10	36.2

failed to reproduce the H-feature. Moreover, the fitting of observed and theoretical LFs became worse with the age spread decreasing. Furthermore, an age spread of order of tens of Myrs could not be attributed to the photometric errors or the effect of unresolved binaries even for low-mass Pleiades stars. The best agreement between a theory and observations is achieved at SFR duration of 60 Myr. According to Table 1, the derived SFR is essentially constant ( $\beta = 0$ ) for the power-law IMF and does not differ significantly from a constant for the log-normal IMF. In this case the average age of Pleiades stars should be about 60 Myrs ( $\log t = 7.78$ ).

There is a long-standing debate on the possibility that stars in a cluster do not have the same ages, especially in the Pleiades. More precisely, there are two separate questions (see Soderblom et al. 1993): First, is there a systematic difference in ages for stars of different masses (age difference)? Second, is there a spread in the ages of stars of the same mass (age spread)?

First evidence for age differences was found by Herbig (1962). He interpreted the lack of evidence for pre-MS evolution in the Pleiades by a significantly higher age of the low-mass stars compared to the high-mass stars. This result was qualitatively confirmed by Iben & Talbot (1966) for other young clusters. More recent discussions, however, have considerably weakened

that evidence (Stahler 1985; Mazzei & Pigatto 1989; Basri et al 1996).

Star formation in stellar aggregates may generally have complex histories, and there is no evidence against an age spread in clusters (Zinnecker et al. 1993). However, as was emphasized by Soderblom et al. (1993), the effects are subtle and we do not have yet a direct measurement for an age spread. In their review on regions of recent star formation, Zinnecker et al. (1993) give an upper limit for the age spread of 10 Myrs. For the Pleiades cluster a limit of 30 Myrs has been derived by Stauffer et al. (1985) and of 20 Myrs by Soderblom et al. (1993). These results are in agreement with the lower limit of 18 Myrs found from the criterion of the visibility of the H-feature. On the other hand, our “best” value of 60 Myrs, seems surprisingly large. A possibility to decrease the derived age spread is to increase the pre-MS evolution scale. This would attach the observed absolute magnitude of the H-feature to older ages reducing thus the age spread necessary for the feature to be visible.

In the present study, the argumentation for an age spread is related to low-mass stars. The presence of the H-feature in the LF leads to the conclusion that low-mass stars are, on average, younger than the cluster age derived from the upper CMD. If true, this result is in qualitative agreement with the picture of cluster formation strongly influenced (and perhaps induced) by the effects of prior massive star formation (e.g. Zinnecker et al. 1993; Larson 1996). However, it seems clear that there are considerable uncertainties in age dating for low-mass stars as well as for high-mass stars (see e.g. the discussion by Basri et al. 1996), and a comprehensive discussion of the age difference problem is clearly beyond the scope of this paper.

## 6. Conclusions

In the present study the LF of Pleiades cluster stars constructed in a previous paper (Meusinger et al. 1996) was revised to investigate its fine structure related to pre-MS stellar evolution. The list of the cluster members was re-considered and the “naive” filter was applied to the LF to reveal its fine structure at faint ( $M_V \geq 5^m$ ) magnitudes. The theoretical LFs based both on post-MS and pre-MS present-day stellar models were constructed. We tested different laws both for the IMF and for the history of the star formation rate.

The following conclusions can be drawn as results of this study:

- The agreement between the observed Pleiades CMD with the new HIPPARCOS distance and the theoretical ZAMS for a normal metallicity is excellent when the model positions in the HRD are corrected to the helium abundance  $Y=0.34$ . The corresponding age of the cluster is  $\log t = 7.95$ .
- Stars fainter than  $M_V = 5.5^m$  have not yet reached the ZAMS.
- There are three features (local peaks followed by dips) found in the cluster LF in a magnitude range  $M_V = 5^m - 12^m$ .
  - \* Two of them (at  $M_V = 7.5^m$  and  $9.5^m$ ) are assumed to be field LF features: Wielen and Kroupa dips. Theoretical models failed to reproduce them.

- \* We attributed the H-feature (the LF detail at  $M_V = 5.5^m$ ) to pre-MS evolution of Pleiades stars.

- The observed Pleiades LF in its brighter part corresponds to the standard Population I IMF. The log-normal IMF describes the observations much better than a simple power-law IMF.
- Assuming that the pre-MS models responsible for H-feature generation, and the current Pleiades age of order of 100 Myrs are correct, the only possibility to interpret the H-feature as a result of pre-MS evolution is to suppose the existence of an age spread for the cluster stars. The required duration of the star formation period is of about several tens of Myrs and the SFR does not depend on time. The significance of this result primarily depends on how strong the appearance of the H-feature may be influenced by unresolved binaries.

The conclusions are based on present-day adopted stellar models (both pre-MS and post-MS) defining the Pleiades age, and the theoretical LF computed on the base of these models.

*Acknowledgements.* It is a pleasure to acknowledge useful discussions with N.V.Kharchenko. We appreciate the useful comments of the referee John R. Stauffer. This research was partly supported by the Deutsche Forschungsgemeinschaft.

## References

- Basri G., Marcy G.W., Graham J.R., 1996, ApJ, 458, 600  
 Belikov A.N., Piskunov A.E., 1997a, Astron.Zh., 74, 34  
 Belikov A.N., Piskunov A.E., 1997b, in preparation  
 D’Antona F., Mazzitelli I., 1994, ApJS 90, 467  
 Duquennoy A., Mayor M., 1991, A&A 248, 485  
 Eichhorn H., 1960, Astron. Nachr., 285, 233  
 Herbig G.H., 1962, ApJ, 135, 736  
 Iben I. Jr., Talbot R. J., 1966, ApJ, 144, 968  
 Kroupa P., Tout C.A., Gilmore G., 1990, MNRAS 224, 76  
 Larson R. B., 1996, In: The interplay between massive star formation, the ISM and galaxy evolution, eds. Kunth D., Guiderdoni B., Heydari-Malayeri M., Thuan T. X., Editions frontieres, Paris, p.3  
 Malkov O.Yu., Piskunov A.E., Shpil’kina D.A., 1997, A&A., 320, 79.  
 Mazzei P., Pigatto L., 1989, A&A, 213, L1  
 Meynet G., Mermilliod J.-C., Maeder A., 1993, A&AS 98, 477  
 Mermilliod J.-C., Turon C., Robichon N., Arenou F., Lebreton Y., 1997, ESA SP-402, 643  
 Meusinger H., Schilbach E., Souchay J., 1996, A&A, 312, 833  
 Piskunov A.E., Malkov O.Yu., 1991, A&A, 247, 87  
 Piskunov A.E., Belikov A.N., 1996, Pis’ma Astron. Zh., 22, 522  
 Röser S., Schilbach E., Hirte S., 1995, ESA SP-379, 143  
 Schaller G., Schaerer D., Meynet G., Maeder A., 1992, A&AS 96, 269  
 Sears R.L., Brownlee R.R., 1965, in: Stellar Structure, eds. Aller L.H., McLaughlin D.B., Chicago  
 Schmidt-Kaler Th., 1982, in: Landolt-Börnstein Numerical Data and Functional Relationships in Science and Technology, New Series, Group VI, eds. Schaifers K., Voigt H. H., New-York, Springer-Verlag, vol.2, p.15  
 Silverman B.W., Density Estimation for Statistics and Data Analysis, Chapman & Hall, London, 1986  
 Soderblom D.R., Stauffer J.R., MacGregor K.B., Jones B.F., 1993, ApJ, 409, 624  
 Stahler S. W., 1985, ApJ, 293, 207

- Stauffer J.R., Hartmann L.W., Burnham J.N., Jones B.F., 1985, *ApJ*, 289, 247
- Zinnecker H., McCaughrean M. J., Wilking B. A., 1993, in: *Protostars and Planets III*, eds. Levy E. H., Lunine J. I., The University of Arizona Press, Tucson, p. 429